

## Ortho Green Fluorescence Protein Synthetic Chromophore; Excited-State Intramolecular Proton Transfer via a Seven-Membered-Ring Hydrogen-Bonding System

Kew-Yu Chen, Yi-Ming Cheng, Cheng-Hsuan Lai, Cheng-Chih Hsu, Mei-Lin Ho, Gene-Hsiang Lee, and Pi-Tai Chou\*

Department of Chemistry, National Taiwan University, Taipei, 106, Taiwan, R.O.C.

Received February 7, 2007; E-mail: chop@ntu.edu.tw

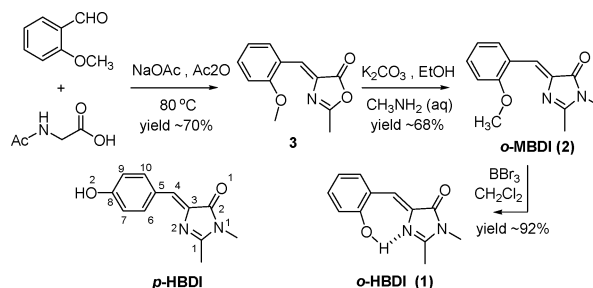
Green fluorescence protein (GFP), which serves as an energy acceptor and emitter for bioluminescence in the sea pansy *Renilla reniformis* and the jellyfish *Aequorea victoria*, has drawn much attention because of its applications in molecular biology and biochemistry.<sup>1</sup> GFP takes advantage of the presence of a chromophore that is anchored both covalently and via a hydrogen-bond network, 4-(4-hydroxybenzylidene)-1,2-dimethyl-1*H*-imidazol-5(4*H*)-one (*p*-HBDI, see Scheme 1), which undergoes excited-state proton transfer (ESPT)<sup>2</sup> via the proton relay of water molecules and a remote residue such as E222,<sup>3</sup> resulting in a very effective and intense anion fluorescence.

Nevertheless, studies reveal a strong cutoff between the properties of wild type GFP (or certain GFP mutants) and the synthetic analogue chromophores of *p*-HBDI.<sup>4</sup> In view of photophysics, the fluorescence yield of the protein-free chromophore in fluid solvents is much weaker and strongly temperature dependent. The results suggest an efficient radiationless transition operating in *p*-HBDI, most probably induced by conformational relaxation along torsional deformation of the two exocyclic C–C bonds to a nonfluorescent twisted intermediate.<sup>5</sup> More recently, it has been proposed that the shallow potential energy surface of the intermediates may conically intersect with that of the ground state, inducing the dominant radiationless deactivation.<sup>4c–d,6</sup> Such a conformational relaxation is greatly suppressed in GFP by its proton relay, rigid environment.

In view of chemistry, most of the research has been focused on the chemical modification of *p*-HBDI analogues at the C(1) position.<sup>4c,7</sup> Conversely, in this study, we are interested in the derivatization on the phenyl ring. As an ingenious approach, switching the hydroxyl group from the C(8) position to the C(6) position (see Scheme 1), forming 4-(2-hydroxybenzylidene)-1,2-dimethyl-1*H*-imidazol-5(4*H*)-one (*o*-HBDI), a structural isomer of *p*-HBDI. The geometry optimization (B3LYP/cc-pVDZ and aug-cc-pVDZ, see ESI) of *o*-HBDI unveils the existence of a seven-membered-ring intramolecular hydrogen bond between –OH and the N(2) atom. This intramolecular hydrogen-bonding configuration should, in part, hinder the exocyclic torsional deformation such that the radiationless deactivation may be reduced. More importantly, theoretical approaches also predict that excited-state intramolecular proton transfer (ESIPT) from the OH proton to the N(2) atom is thermally favorable (vide infra), forming a zwitterionic tautomer species (see Table of Content, TOC).

In light of these perspectives, we have thus expended great effort to make a facile synthesis of *o*-HBDI. Briefly, the *o*-methoxybenzaldehyde was used as a starting reactant (see Scheme 1). Because of the lack of the *o*-hydroxyl group and hence the intramolecular lactonation, **3** was obtained with a good yield (70%). Subsequent reaction of **3** with methylamine, followed by deprotection of the methyl group of *o*-MBDI by BBr<sub>3</sub>, afforded *o*-HBDI with an overall

### Scheme 1. The Synthesis of *o*-HBDI and the Structure of *p*-HBDI<sup>a</sup>



<sup>a</sup> The Non-IUPAC atom label is for the convenience of discussion.

product yield of 43%. Detailed synthetic procedures and product characterization are provided in ESI.

The structure of *o*-HBDI was further confirmed by single-crystal X-ray diffraction analysis. As depicted in Figure 1, the nearly planar configuration between phenol and imidazolidinone rings was established by  $\angle N(2)-C(3)-C(5)-C(6)$  of  $-1.05^\circ$ . This, together with 2.63 Å of O(2)–N(2) distance and  $176^\circ$  of  $\angle N(2)-H-O(2)$ , strongly supports the seven-membered-ring intramolecular hydrogen-bonding formation. In good agreement with this observation, the <sup>1</sup>H NMR spectrum (in CDCl<sub>3</sub>) revealed a significantly downfield signal at  $\delta$ 13.7, giving a clear indication of the strong hydrogen-bond formation.

Figure 2 shows the absorption and emission spectra of *o*-HBDI in cyclohexane. The absorption is characterized by a lowest-energy absorption band maximized at 385 nm, for which the  $\epsilon$  value of  $(2.0 \pm 0.3) \times 10^4 \text{ M}^{-1} \text{ cm}^{-1}$  makes its assignment to the  $\pi \rightarrow \pi^*$  transition unambiguous. The steady-state emission consists solely of one band maximized at as long as 605 nm with a moderate quantum yield of  $(3.1 \pm 0.2) \times 10^{-3}$ . To further verify the origin of the emission, *o*-MBDI, (see Scheme 1), was also investigated. Owing to its lack of a hydroxyl proton, *o*-MBDI serves as a model to represent the prohibition of the proton-transfer reaction. As depicted in Figure 2, the  $S_0 \rightarrow S_1$  absorption ( $\lambda_{\text{max}} \approx 370 \text{ nm}$ ) and the corresponding emission peak wavelength ( $\lambda_{\text{max}} \approx 425 \text{ nm}$ ) for *o*-MBDI reveal a mirror image with a normal Stokes shift.

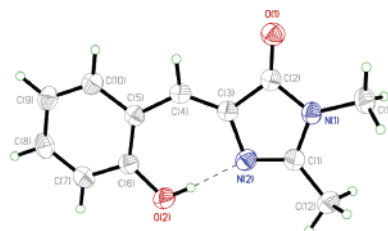
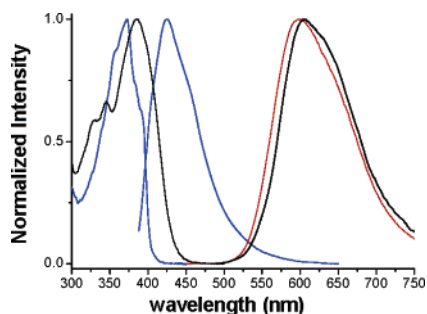


Figure 1. The molecular structure of *o*-HBDI, thermal ellipsoids drawn at the 50% probability level.



**Figure 2.** The absorption and emission spectra of *o*-HBDI in cyclohexane (black solid line) and solid film (red solid line, emission only) and *o*-MBDI (blue solid line) in cyclohexane.

Accordingly, the  $\sim 605$  nm emission in *o*-HBDI with an anomalously large Stokes shift (peak-to-peak) of  $\sim 10000$   $\text{cm}^{-1}$  relative to the  $S_0 \rightarrow S_1$  absorption, is unambiguously ascribed to a tautomer emission resulting from the ESIPT reaction, most probably via the phenolic proton to the N(2) nitrogen, forming a zwitterionic species (see TOC for structure). With a femtosecond fluorescence up-conversion technique, the population decay of the 605-nm emission band was measured to be  $32 \pm 0.2$  ps, while the corresponding rise time was beyond the system response of 150 fs, which consists with the system response limited decay time monitored at 450 nm, presumed to be the origin of normal emission.

To further gain insights into the ESIPT kinetics, the H-deuterated O–D compound of *o*-HBDI, *o*-*d*BDI, was also prepared (see Supporting Information) and investigated. Under the same experimental condition as that performed for *o*-HBDI, the up-converted tautomer emission in *o*-*d*BDI also revealed a system response limited rise time and a population decay of  $33 \pm 0.3$  ps. The results demonstrate that the rate of ESIPT is quite insensitive to an H/D exchange and point to an essentially barrierless potential energy surface along the ESIPT reaction. Further support was also given by the theoretical approach. Based on the time dependent DFT method (TDDFT/B3LYP/cc-pVDZ and aug-cc-pVDZ) implemented in the TURBOMOLE 5.8 software package<sup>9</sup> (see SI), the ESIPT process was calculated to be thermally favorable by  $\sim 7.8$  kcal/mol (see TOC). Moreover, upon Franck–Condon excitation and execution of the geometry relaxation, the TDDFT method could not locate the energy minimum of the excited normal species, a result which is consistent with a barrierless ESIPT process concluded experimentally.

As compared to those generally observed weak emissions for *p*-HBDI ( $\Phi_f \approx 10^{-4}$  and  $\tau_f \approx 1.7$  ps in toluene) at room temperature,<sup>4d</sup> the tautomer emission yield of  $3.1 \times 10^{-3}$  with  $\tau_f \approx 32$  ps in cyclohexane implies that the hydrogen-bonding strength may, in part, hinder the exocyclic C–C bonds rotation. Further support is rendered by the much weaker normal emission ( $\Phi_f \approx 5 \times 10^{-4}$  and  $\tau_f \approx 4$  ps in cyclohexane, see Table 1) in *o*-MBDI that lacks the seven-hydrogen bond formation. Nevertheless, the somewhat weak proton-transfer tautomer emission may indicate the active operation of the conformational relaxation owing to the loose rigidity of the seven-membered-ring hydrogen bond. Note that ESIPT still takes place in the solid film (vapor deposition onto a quartz plate) of *o*-HBDI (Figure 2), resulting in a  $\sim 595$  nm tautomer emission with  $\Phi_f$  as high as 0.4 ( $\tau_f \approx 1.7$  ns).

As listed in Table 1, similar ultrasfast ESIPT was also observed, giving a unique tautomer emission, in all aprotic solvents. However, in protic solvent such as water (pH = 7), dual emission, consisting of normal ( $\sim 495$  nm) and tautomer ( $\sim 600$  nm) emission, was

**Table 1.** The Photophysical Properties of *o*-HBDI and *o*-MBDI in Various Solvents at Room Temperature

	<i>o</i> -HBDI				<i>o</i> -MBDI			
	$\lambda_{\text{abs}}^a$	$\lambda_{\text{em}}^a$	$\Phi_f \times 10^{-3}$	$\tau^b$	$\lambda_{\text{abs}}^a$	$\lambda_{\text{em}}^a$	$\Phi_f \times 10^{-4}$	$\tau^b$
C <sub>6</sub> H <sub>12</sub>	385	605	3.1	32.0	372	425	5.0	4.0
CH <sub>2</sub> Cl <sub>2</sub>	386	603	2.2	16.0	374	435	3.1	2.4
CH <sub>3</sub> CN	383	602	1.5	7.9	374	435	2.6	2.2
H <sub>2</sub> O (pH = 7)	380	495	0.9 <sup>c</sup>	0.9	375	460	0.9	0.7
		600		3.2				
H <sub>2</sub> O (pH = 12)	445	580	1.0	12.7				

<sup>a</sup> Unit: nm. <sup>b</sup> Unit: ps. <sup>c</sup> Sum of the dual emission.

resolved (see SI). The result in water can plausibly be rationalized by the partial rupture of the intramolecular hydrogen bond,<sup>10</sup> resulting in the prohibition of ESIPT. This viewpoint can be supported by the lack of correlation between the finite decay of normal emission (0.9 ps, Table 1) and system response limited-rise dynamics of the tautomer ( $< 150$  fs). In pH = 12, the *o*-HBDI anion exhibits absorption and emission at 445 and 580 nm, respectively. Comparing the anionic species, the red shift of the zwitterionic emission can be rationalized by the reduction of electron donating strength at the protonated N(2) nitrogen, resulting in a decrease of the LUMO energy.

To sum up, we have synthesized a structural isomer of the core chromophore (*p*-HBDI) in GFP. *o*-HBDI possesses a seven-membered-ring hydrogen bond, from which ultrafast ESIPT takes place, resulting in a proton-transfer tautomer emission of  $\sim 605$  nm in nonpolar solvents. Although the bioactivity of *o*-HBDI is pending further exploration, its future chemical derivation is versatile. It is believed that fine tuning the proton-transfer emission can be achieved via the derivation at the C(1) position, while the radiationless quenching process may be further reduced by anchoring bulky groups at the C(4) position, generating a new series of isomers of *p*-HBDI with remarkable ESIPT properties.

**Supporting Information Available:** Details for experimental procedures, spectroscopic data, and X-ray studies. This material is available free of charge via the Internet at <http://pubs.acs.org>.

## References

- (1) (a) Chalfie, M.; Tu, Y.; Euskirchen, G.; Ward, W. W.; Prasher, D. C. *Science* **1994**, *263*, 802. (b) Lippincott-Schwartz, J.; Patterson, G. H. *Science* **2003**, *300*, 87. (c) Ormo, M.; Cubitt, A. B.; Kallio, K.; Gross, L. A.; Tsien, R. Y.; Remington, S. J. *Science* **1996**, *273*, 1392. (d) Zimmer, M. *Chem. Rev.* **2002**, *102*, 759. (e) Tsien, R. Y. *Annu. Rev. Biochem.* **1998**, *67*, 509. (f) Sullivan, K. F.; Kay, S. A. *Green Fluorescent Proteins*; Academic Press: San Diego, CA, 1999.
- (2) (a) Hosoi, H.; Mizuno, H.; Miyawaki, A.; Tahara, T. *J. Phys. Chem. B* **2006**, *110*, 22853. (b) Agmon, N. *Biophys. J.* **2005**, *88*, 2452. (c) Stoner-Ma, D.; Jaye, A. A.; Matousek, P.; Towrie, M.; Meech, S. R.; Tonge, P. *J. Am. Chem. Soc.* **2005**, *127*, 2864.
- (3) Stoner-Ma, D.; Melief, E. H.; Nappa, J.; Ronayne, K. L.; Tonge, P. J.; Meech, S. R. *J. Phys. Chem. B* **2006**, *110*, 22009.
- (4) (a) Dong, J.; Solntsev, K. M.; Tolbert, L. M. *J. Am. Chem. Soc.* **2006**, *128*, 12038. (b) Brejc, K.; Sixma, T. K.; Kitts, P. A.; Kain, S. R.; Tsien, R. Y.; Orm, M.; Remington, S. J. *Proc. Natl. Acad. Sci. U.S.A.* **1997**, *94*, 2306. (c) Litvinenko, K. L.; Webber, N. M.; Meech, S. R. *J. Phys. Chem. A* **2003**, *107*, 2616. (d) Mandal, D.; Tahara, T.; Meech, S. R. *J. Phys. Chem. B* **2004**, *108*, 1102.
- (5) (a) Stavrov, S. S.; Solntsev, K. M.; Tolbert, L. M.; Huppert, D. *J. Am. Chem. Soc.* **2006**, *128*, 1540. (b) Gepshtein, R.; Huppert, D.; Agmon, N. *J. Phys. Chem. B* **2006**, *110*, 4434. (c) Usman, A.; Mohammed, O. F.; Nibbering, E. T. J.; Dong, J.; Solntsev, K. M.; Tolbert, L. M. *J. Am. Chem. Soc.* **2005**, *127*, 11214.
- (6) (a) Webber, N. M.; Litvinenko, K. L.; Meech, S. R. *J. Phys. Chem. B* **2001**, *105*, 8036.
- (7) He, X.; Bell, A. F.; Tonge, P. *J. Org. Lett.* **2002**, *4*, 1523.
- (8) He, X.; Bell, A. F.; Tonge, P. *J. Phys. Chem. B* **2002**, *106*, 6056.
- (9) Ahlrichs, R.; Bar, M.; Haser, M.; Hom, H.; Kolmel, C. *Chem. Phys. Lett.* **1989**, *162*, 165.
- (10) McMorro, D.; Kasha, M. *J. Phys. Chem.* **1984**, *88*, 2235.

JA070880I